INTERNATIONAL JOURNAL OF SCIENTIFIC & ENGINEERING RESEARCH, VOLUME 12, ISSUE 4, APRIL-2021
ISSN 2229-5518

Analysis of the Impact of Relative Humidity and Mineral Accumulation Mode Aerosols Particle Concentration on the Visibility and particle size distribution of Desert Aerosols

Yerima S. U[1], Abdulkarim U. Y[2], Tijjani B. I[3], Gana U. M[3], Sani M[4], Aliyu R[5], Abdulhadi D[6], Shamsuddeen M. F[7]

ABSTRACT - This paper presents the results of the Analysis of the Impact of relative humidity and mineral (accumulation mode, nonspherical) MIAN aerosol particles concentrations on the visibility and particle size distribution of desert aerosols based on microphysical properties of desert aerosols. The microphysical properties (the extinction coefficients, volume mix ratios, dry mode radii and wet mode radii) were extracted from Optical Properties of Aerosols and Clouds (OPAC 4.0) at eight relative humidities (00 to 99%RH) and at the spectral range of 0.4-0.8 mm, the concentrations of mineral (accumulation mode, nonspherical) MIAN were varied to obtain five different models. The Angstrom exponent (α), the turbidity (β), the curvature (α_2), humidification factor (γ), the mean exponent of aerosol growth curve (μ) and the mean exponent of aerosol size distributions (υ) were determined from the regression analysis of some standard equations. It was observed that the values of (α) are less than 1 throughout the five models at all RHs which signifies the dominance of coarse mode particles over fine mode particles. But the increase in the magnitude of (α) across the five models signifies the emergence of fine mode particles over the coarse mode particles. It was observed that the curvature (α_2) has both negative signs (monomodal) and positive signs (bimodal) types of distributions all through the five models and this signifies the dominance of coarse mode particles with some traces of fine mode particles across the individual models. The visibility was observed to decrease with the increase in RH and increased with wavelength. The analysis further found that there is an inverse power law relationship between humidification factor, the mean exponent of the aerosol size distribution with the mean exponent of the aerosol growth curve (as the magnitude of (μ) increases across the five models, the magnitudes of (γ) and (υ) decreased, but the magnitude of both (γ) and (υ) decreased with the increase in wavelength for a given (μ) across the individual models). The mean exponent of aerosol size distribution (υ) being less than 3 indicate foggy condition of the desert atmosphere.

Index Terms: Extinction coefficient, Visibility Enhancement parameter, Hygroscopic growth, mean exponent of the aerosol size distribution, humidification factor, mean exponent of the aerosol growth curve

1 INTRODUCTION

Atmospheric aerosols are known to change the climate transformation but they still constitute one of the largest uncertainties in climate change studies [1]. Aerosols change the Earth's climate directly by scattering or absorbing solar radiation and indirectly by modifying the cloud characteristics [2]. Mineral dust are mainly obtained from Desert which spread across the desert atmosphere [3]. There particles have serious effect on both regional and global climate through their interaction with solar and terrestrial radiation [4]. Desert aerosols particles exhibit hygroscopic growth due to chemical transformations and water uptake which occurred during long-range transport [1].

Atmospheric aerosols, which are defined as liquid or solid particles suspended in a gas [5], are very tiny and usually can't be seen by our eyes. Nevertheless, they have a serious influence on our health and global climate at large. Aerosols directly influence the Earth's radiation budget by scattering and absorbing solar radiation [6]. In addition, anthropogenic aerosol particles modify cloud properties and changed precipitation behavior [7].

Aerosol particles absorb water, as such they change in size and chemical composition depending on the ambient relative humidity (RH) and subsequently these affect the visibility[8], as such proper studies of the effects of varying the RHs on aerosols optical and microphysical properties are usually performed at standardized conditions to avoid under estimating the RH effect when characterizing the main aerosol properties [9]. However, knowledge of the impact of

[1] Nigerian Meteorological Agency (NIMET), Nnamdi Azikwe International Airport Abuja.
sunusiyerima@yahoo.com, sunusiyerima86@gmail.com
+234 8037335747
[2]Department of Physics, Saadatu Rimi Collage of Education Kano, Kano State, Nigeria.
[3]Department of Physics, Bayero University Kano, Kano State, Nigeria.
[4]Center for Atmospheric Research, National Space Research and Development Agency (NARSDA), Anyigba, Nigeria.
[5]Department of Physics, Kano State University of Science and Technology Wudil, Kano State, Nigeria.
[6] Department of Science Laboratory Technology, Nuhu Bamalli Polytechnic Zaria, Kaduna State Nigeria.
[7] Department of Remedial and General Studies, Audu Bako Collage of Agriculture Danbatta Kano State Nigeria.

INTERNATIONAL JOURNAL OF SCIENTIFIC & ENGINEERING RESEARCH, VOLUME 12, ISSUE 4, APRIL-2021
ISSN 2229-5518

varying the concentration of mineral accumulation mode and relative humidity on visibility is very crucial.

Particles in the atmosphere arise from natural sources, such as windborne dust, sea spray, volcanoes, and from anthropogenic activities, such as combustion of fuels. Whereas an aerosol is technically defined as a suspension of fine solid or liquid particles in a gas [6], Mineral dust particles can travel long distances and coagulate with soluble sulphates, nitrates and other electrolytes transported over polluted desert atmosphere [10].

In this paper the extinction coefficients, volume mix ratios, dry mode radii and wet mode radii of desert aerosols were extracted from OPAC (4.0) at the spectral wavelength of 0.4 to 0.8μm, and at relative humidities of 00-99%. In OPAC 4.0, the desert aerosols are modeled using four compositions of aerosols as water soluble (WASO), Mineral transported (nuclei mode, nonspherical) MINN, mineral (coarse mode, nonspherical) MICN and mineral (accumulation mode, nonspherical) MIAN. From the four components of the aerosols, the MIAN concentration was varied. The data were analyzed using excel, SPSS, Origin and uses some standard formulae. The effective hygroscopic growth, humidification factor, visibility enhancement parameter, visibility, the mean exponent of aerosol growth curve and the mean exponent of aerosol size distribution were determined.

2.0 METHODOLOGY

Table 1 shows the models components of the compositions of the desert aerosols used to determine the extinction coefficients of the mixture.

Table1: The models used in the simulations of the desert aerosols.

	Model1	Model2	Model3	Model4	Model5
Comp	No. Den. (cm^{-3})	No. Den. (cm^{-3})	No. Den. (cm^{-3})	No. Den. (cm^{-3})	No. Den. (cm^{-3})
WASO	2000	2000	2000	2000	2000
MINN	269.5	269.5	269.5	269.5	269.5
MIAN	40.5	50.5	60.5	70.5	80.5
MICN	0.142	0.142	0.142	0.142	0.142

An objective measure of visibility is the standard visual range or meteorological range [11].

$$Vis(\lambda) = \frac{3.912}{\sigma_{ext}(\lambda)} \quad (1)$$

Meteorological range refers to the visual range of a black object seen against its surrounding [12]. The visual extinction coefficient $\sigma_{ext}(\lambda)$ is the measure of light scattering and absorbing properties of the atmosphere along the line of sight [13]. To determine the visibility using the extracted extinction coefficient, the variation of the extinction coefficient with wavelength was determined using the inverse power law of extinction coefficient as;

$$\sigma_{ext}(\lambda) = \beta\lambda^{-\alpha} \quad (2)$$

where α and β are known as Angstrom parameters. The index α is the wavelength exponent or Angstrom coefficient and β is the turbidity coefficient representing the amount of aerosols present in the atmosphere in the vertical direction or the total aerosol loading in the atmosphere [14],[15].

Substituting equation (2) into (1), the following equation is obtained which is the variation of the visibility with wavelength.

$$Vis(\lambda) = \frac{3.912}{\beta}\lambda^{\alpha} \quad (3)$$

Equation (3) can also be written as

$$ln\left(\frac{Vis_{\lambda}}{3.912}\right) = -ln(\beta) + \alpha\, ln(\lambda) \quad (4)$$

To obtain α (slope) and β (intercept) a regression analysis was performed using an expression derived from the Kaufman (1993) representation of the equation [16].

However, The Angstrom exponent itself varies with wavelength, and a more precise empirical relationship between visibility and wavelength is obtained with a 2nd-order polynomial [17],[21]

$$ln\left(\frac{Vis_{\lambda}}{3.912}\right) = -ln(\beta) + \alpha_1 ln(\lambda) + \alpha_2\left(ln(\lambda)\right)^2 \quad (5)$$

Here, the coefficient α2 accounts for a "curvature" often observed in the sun photometry measurements. Some authors have noted that the curvature is also an indicator of the aerosol particle size, with negative curvature indicating aerosol size distributions dominated by the fine mode and positive curvature indicating size distributions with a significant coarse mode contribution [22], [25].

Now, to determine the relationship between visibility and relative humidity, enhancement parameter is defined as [26].

$$f(RH,\lambda) = \frac{Vis(RH,\lambda)}{Vis(RH=0,\lambda)} = \left[\frac{1-(RH)}{1-(RH=0)}\right]^{-\gamma} \quad (6)$$

Now taking the natural log of both side we have

$$ln\left(\frac{Vis(RH,\lambda)}{Vis(0,\lambda)}\right) = -\gamma ln(1-RH) \quad (7)$$

Also, γ is given as (Tijjani, 2013)

$$\gamma = \frac{(\upsilon-1)}{\mu} \quad (8)$$

where γ is the humidification factor representing the dependence of visibility on RH, It arises from the change in the particle size and refractive indices upon humidification [18,28]. The use of γ has an advantage of describing the hygroscopic behavior of visibility in a linear manner over a broad range of RH values, and also implies that particles are deliquesced [28], the γ parameter is dimensionless, and it increases with increase in particle water uptake [9]. μ is defined as the mean exponent of the aerosol growth curve constant, υ as the mean exponent of the aerosol size distribution [26].

Junge have demonstrated the need for using logarithmic range for the interpretation of the mean exponent of the aerosol size distributions [29]. Based on experimental observations, he proposed a power law size distribution function of the form;

$$\frac{dn(r)}{d(logr)} = Cr^{-\upsilon} \quad (9)$$

INTERNATIONAL JOURNAL OF SCIENTIFIC & ENGINEERING RESEARCH, VOLUME 12, ISSUE 4, APRIL-2021
ISSN 2229-5518

where dn(r) is the number of particles with radii between r and r+dr, C is constant depending on the number of particles in one cubic centimeter and the exponent υ determines the mean exponent of aerosol size distribution. As υ values decrease the number of larger particles increases compared to smaller particles [24].

Now, the hygroscopic growth g(RH) experienced by a single aerosol particle according to [26] is given by

$$g(RH) = \frac{r(RH)}{r(RH=0)} \quad (10)$$

where r(RH) is the radius at RH% and r(RH=o) is the radius at 0%RH.

Now, the effective hygroscopic growth of the four components of the aerosols is given as:

$$g_{eff}(RH) = \left(\sum_i x_i g_i^3(RH)\right)^{\frac{1}{3}} \quad (11)$$

where the summation is performed over all compounds present in the particles and x_i represents the respective volume fraction of single aerosol particle concentration and g_i is the hygroscopic growth of the i^{th} aerosol particles using the Zdanovskii-Stokes-Robinson relation [30], and i= 1,2,3,4.

Now, the relationship between effective hygroscopic growth and RH is expressed as:

$$g_{eff}(RH) = \left[\frac{1-(RH)}{1-(RH=0)}\right]^{-\frac{1}{\mu}} \quad (12)$$

where μ is defined as the mean exponent of the aerosol growth curve constant as defined in equation (8) equation (12) can be written as:

$$\ln g_{eff}(RH) = -\frac{1}{\mu}\ln(1-RH) \quad (13)$$

Now, expressing υ (the mean exponent of the aerosol size distribution) in terms of μ and γ (the humidification factor) using equations (8) and (11) we have:

$$\nu = \gamma\mu + 1 \quad (14)$$

3.0 Results and Discussions

This section presents the results of the analyzed data extracted from OPAC 4.0 based on the models presented in table1

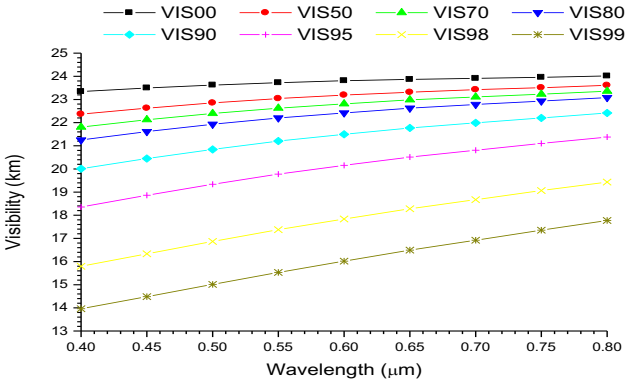

Fig. 1 a graph of visibility against wavelength for Mian model 1

From Fig. 1, it can be observed that the visibility increases with the increase in wavelength, and decreases with the increase in relative humidity (RH). It can also be observed that the visibility is lower at shorter wavelengths with maximum and minimum values of 23.4km and 13.9km respectively. This shows the dominance of coarse mode particles with some traces of fine mode particles. It should also be noted that fine mode particles scatter and absorb more solar radiation than the coarse mode particles [31]. Since from equation (3) the visibility is the inverse of extinction, this implies that the visibility will be lower at shorter wavelengths. The change in visibility is more pronounced from 90%RH to 99%RH.

Table 2 Results of the regression analysis of equations (4) and (5) for visibility using SPSS.

	Linear			Quadratic			
RH	R^2	α	β	R^2	α_1	α_2	β
0%	0.853927	0.033923	0.161785	0.907676	0.014641	-0.043067	0.16366
50%	0.963507	0.078151	0.162632	0.966590	0.052932	-0.022367	0.163608
70%	0.979482	0.101566	0.163125	0.981607	0.074572	-0.023940	0.164173
80%	0.964302	0.118551	0.164549	0.989853	0.008444	-0.097649	0.168904
90%	0.996943	0.175504	0.166678	0.997876	0.144870	-0.027168	0.167894
95%	0.997265	0.221988	0.173406	0.997508	0.202203	-0.017547	0.174222
98%	0.999057	0.291584	0.189206	0.999060	0.294414	0.0025132	0.189079
99%	0.998812	0.349628	0.204293	0.998886	0.368064	0.0163587	0.203401

By observing the R^2 values from both the linear and quadratic part of Table 2, it can be seen that the data fitted the equation models very well. From the linear part, since α (angstrom exponent) is less than 1, this signifies the dominance of coarse mode particles. The increase of α with RH shows that coarse mode particles are being reduced from the atmosphere more than fine mode particles as a result of the increase in RH due to coagulation and sedimentation. Considering the quadratic part, it can be seen that $\alpha 2$ is negative from RH of 0 to 95%, and this shows monomodal distribution of coarse mode particles. But from the RH of 98% to 99% it changed to positive and this indicates bimodal type of distribution with coarse mode particles as dominant and traces of fine mode particles. The fluctuations of the magnitudes of α_2 with RH shows the non-linearity relation between particles size distribution and RH and also with the physically mixed aerosols. The increase in turbidity coefficient β with RH signifies decrease in visibility with increase in RH.

Table 3 the result of the analysis of equations (8) and (12) using SPSS.

	μ	14.09622	
λ(m)	R^2	γ	υ
0.55	0.947681	0.075146	2.059275
0.65	0.938553	0.064349	1.907078
0.75	0.930637	0.055208	1.778224

By observing the values of R^2, it can be said that the data fitted the equation models very well. Equation (6) shows that the

visibility enhancement factor satisfies the inverse power law with (1-RH). The decrease of humidification factor with wavelength also shows that the visibility increases with the increase in wavelength. Equation (12) shows that the hygroscopic growth has satisfied the inverse power relation also with (1-RH) and the reciprocal of mean exponent of aerosol growth curve. It can also be said that for a fixed value of mean exponent of the aerosol growth curve μ, the humidification factor γ decreases with the increase in wavelength, this also shows that the visibility increases with the increase in wavelength (as the particles size decreases) i.e it satisfies the inverse power law of equation (6) and decreases with an increase in RH. Based on equation (9), the mean exponent of the aerosol size distribution (v) decrease with wavelength which shows that the number of larger particles increase compared to smaller particles and this is due to major coagulation amount caused by the increase in number of fine mode particles and consequently the tiny particles coagulate more than the larger particles as said by [29],[32]. It can also be noted from the values of (v) that the average atmospheric condition of the area is foggy [29].

Table 4 the results of the analysis of skewness and kurtosis using SPSS.

	Invis00	Invis50	Invis70	Invis80	Invis90	Invis95	Invis98	Invis99
Skewness	-0.8248	-0.5438	-0.4458	-0.7698	-0.4062	-0.3626	-0.3080	-0.2832
Kurtosis	-1.0794	-0.1795	-1.0936	-0.6573	-1.0516	-1.1018	-1.1393	-1.1308

From Table 4, the behaviors and changes of particles size distribution are displayed in terms of vertical behavior (kurtosis) and horizontal behavior (skewness). From skewness, it can be seen that it is negative all through, this implies that it is negatively skewed and this signifies that the particle distribution is dominated by coarse mode particles. From the kurtosis, it can be observed that it is also negative all through, and this shows that it is platykurtic, and the average vertical size distribution of the particles is below normal size distribution. The fluctuations in the values of the values of skewness and kurtosis maybe due to the nonlinear relation between the particles size distribution with RH and the physically mixed aerosols.

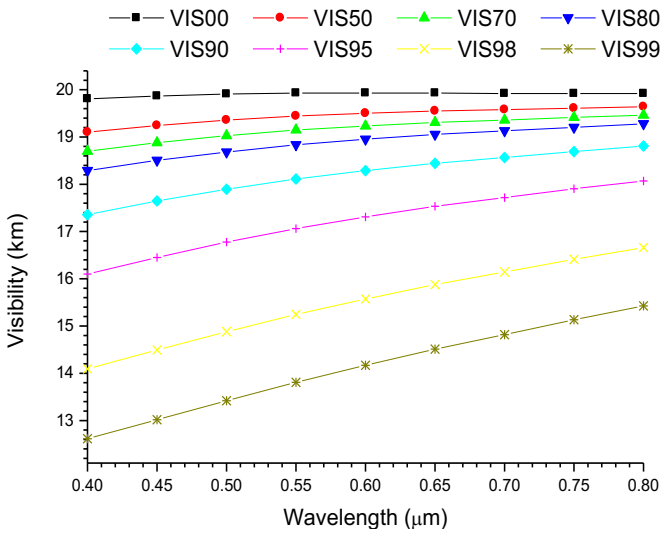

Fig. 2 a graph of visibility against wavelength for mian model 2

From Fig. 2, it can be observed that the visibility increases with the increase in wavelength, and decreases with the increase in relative humidity (RH). It can also be observed that the visibility is lower at shorter wavelengths with the maximum and minimum values of 19.9km and 12.8km which shows the dominance of coarse mode particles with some traces of fine mode particles. It should also be noted that fine mode particles scatter and absorb more solar radiation than the coarse mode particles [31]. Since from equation (3) the visibility is the inverse of extinction, this implies that the visibility will be lower at shorter wavelengths. It can also be noted that the variation in the visibility at lower RHs (00-80) and higher wavelengths is very sharp but it is more pronounced at the higher RHs.

Table 5 Results of the regression analysis of equations (4) and (5) for visibility using SPSS.

	Linear			Quadratic			
RH	R^2	α	β	R^2	α_1	α_2	β
0%	0.366586	0.008555	0.195251	0.718639	0.039281	-0.042424	0.197480
50%	0.853927	0.033923	0.197605	0.907676	0.014640	-0.043067	0.199895
70%	0.911931	0.059966	0.197925	0.982095	0.034949	-0.084168	0.202433
80%	0.983543	0.084078	0.198230	0.987011	0.055593	-0.025263	0.199575
90%	0.988994	0.111533	0.202635	0.993504	0.068558	-0.038113	0.204712
95%	0.989134	0.166572	0.207994	0.996135	0.086610	-0.070916	0.211978
98%	0.998293	0.241554	0.222305	0.998760	0.211749	-0.026433	0.223883
99%	0.999057	0.291584	0.238135	0.999060	0.294414	0.002510	0.237975

By observing the R^2 values from both the linear and quadratic part of Table 5, it can be seen that the data fitted the equation models very well from the 50%RH to 99%RH but weakly correlated at 00%RH. From the linear part, since α (angstrom exponent) is less than 1, this signifies the dominance of coarse mode particles over fine mode particles. The increase of α with RH shows that coarse mode particles are being reduced from

INTERNATIONAL JOURNAL OF SCIENTIFIC & ENGINEERING RESEARCH, VOLUME 12, ISSUE 4, APRIL-2021
ISSN 2229-5518

the atmosphere more than fine mode particles due to coagulation and sedimentation. Considering the quadratic part, it can be seen that α_2 is negative from RH of 0 to 98%, and this shows monomodal distribution of coarse mode particles. But at RH of 99% it changed to positive and this indicates bimodal type of distribution with coarse mode particles as dominant and traces of fine mode particles. The fluctuations in α_2 with RH shows the non-linearity relation between particles size distribution and RH and also with the physically mixed aerosols. The increase in turbidity coefficient β with RH signifies decrease in visibility with increase in RH.

Table 6 the result of the analysis of equations (8) and (12) using SPSS.

	μ	15.57244	
λ(m)	R^2	γ	v
0.55	0.945269	0.064713	2.00774
0.65	0.935492	0.054884	1.854678
0.75	0.927849	0.046824	1.729164

By observing the values of R^2, it can be said that the data fitted the equation models very well. Equation (6) shows that the visibility enhancement factor satisfies the inverse power law with (1-RH). The decrease of humidification factor with wavelength also shows that the visibility increases with the increase in wavelength. Equation (12) shows that the hygroscopic growth has satisfied the inverse power relation also with (1-RH) and the reciprocal of mean exponent of aerosol growth curve. It can also be said that for a fixed value of mean exponent of the aerosol growth curve μ, the humidification factor γ decreases with the increase in wavelength, this also shows that the visibility increases with the increase in wavelength (as the particles size decreases) i.e it satisfies the inverse power law of equation (6) and decreases with an increase in RH. Based on equation (9), the mean exponent of the aerosol size distribution (v) decrease with wavelength which shows that the number of larger particles increase compared to smaller particles and this is due to major coagulation amount caused by the increase in number of fine mode particles and consequently the tiny particles coagulate more than the larger particles as said by [29],[32]. It can also be noted from the values of (v) that the average atmospheric condition of the area is foggy [29].

Table 7 the results of the analysis of skewness and kurtosis using SPSS.

	Invis00	Invis50	Invis70	Invis80	Invis90	Invis95	Invis98	Invis99
Skewness	-3.0000	-0.8248	-0.9985	-0.4687	-0.5265	-0.6062	-0.3810	-0.3080
Kurtosis	9.0000	-1.0794	-0.1871	-0.8438	-0.6429	-0.4530	-0.8978	-1.1393

From Table 4, the behaviors and changes of particles size distribution are displayed in terms of vertical behavior (kurtosis) and horizontal behavior (skewness). From skewness, it can be seen that it is negative from the RHs of 00 to 99%, this implies that it is negatively skewed and this signifies that the particle size distribution is dominated by coarse mode particles. From the kurtosis, it can be observed that it is also negative all through. and this shows that it is platykurtic, and the average vertical size distribution of the particles is below normal size distribution. The fluctuations in the values of the values of skewness and kurtosis maybe due to the nonlinear relation between the particles size distribution with RH and the physically mixed aerosols.

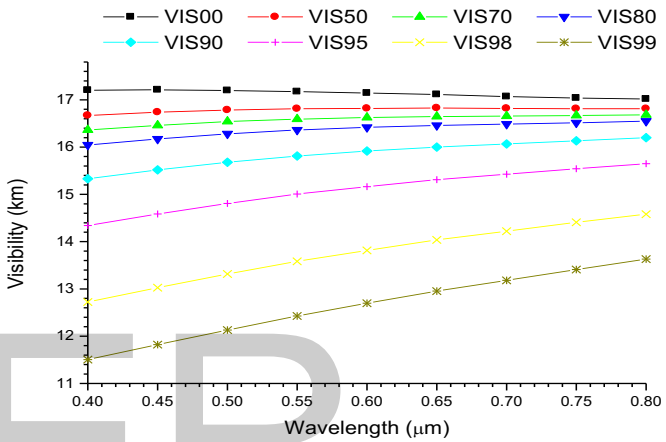

Fig. 3 a graph of visibility against wavelength for mian model 3

From Fig. 3, it can be observed that the visibility increases with the increase in wavelength, and decreases with the increase in relative humidity (RH). It can also be observed that the visibility is lower at shorter wavelengths with the maximum and minimum values of 17.2km and 11.75km which shows the dominance of coarse mode particles with some traces of fine mode particles. It should also be noted that fine mode particles scatter and absorb more solar radiation than the coarse mode particles [31]. Since from equation (3) the visibility is the inverse of extinction, this implies that the visibility will be lower at shorter wavelengths. It can also be noted that the variation in the visibility at lower RHs (00-80) and higher wavelengths is very sharp but it is more pronounced at the higher RHs.

Table 8 Results of the regression analysis of equations (4) and (5) for visibility using SPSS.

	Linear			Quadratic			
RH	R^2	α	β	R^2	α_1	α_2	β
0%	0.610554	0.01656	0.230431	0.813849	0.071090	-0.04836	0.233432
50%	0.600290	0.014482	0.230956	0.829863	0.036622	-0.04532	0.233774
70%	0.826478	0.027996	0.232370	0.892933	0.017301	-0.04017	0.234881
80%	0.880885	0.041937	0.233739	0.947073	0.023651	-0.05817	0.237405
90%	0.975779	0.072526	0.237210	0.982958	0.037031	-0.03148	0.239216
95%	0.995232	0.124094	0.242854	0.995768	0.140529	0.014575	0.241909
98%	0.996515	0.201956	0.256017	0.996675	0.216561	0.012953	0.255131
99%	0.997097	0.241100	0.272195	0.997102	0.237965	-0.00278	0.272397

By observing the R^2 values from both the linear and quadratic part of Table 8, it can be seen that the data fitted the equation models very well from the RH of 70% to 99% but poorly fitted from 00%RH to 50%RH. From the linear part, since α (angstrom exponent) is less than 1, this signifies the dominance of coarse mode particles. The increase of α with RH shows that coarse mode particles are being reduced from the atmosphere more than fine mode particles as a result of the increase in RH and also due to coagulation and sedimentation. Considering the quadratic part, it can be seen that α_2 is negative at all RHs except at 95% and 98%, and this shows monomodal distribution of coarse mode particles except at 95% and 98% which is bimodal distribution of coarse mode particles. The fluctuations in the magnitude of α_2 with RH shows the non-linearity relation between particles size distribution and RH and also with the physically mixed aerosols. The increase in turbidity coefficient β with RH signifies decrease in visibility with increase in RH.

Table 9 the result of the analysis of equations (8) and (12) using SPSS.

	μ	17.02359	
λ(m)	R^2	γ	v
0.55	0.942339	0.056689	1.965051
0.65	0.934143	0.047976	1.816724
0.75	0.92571	0.040599	1.691141

By observing the values of R^2, it can be said that the data fitted the equation models very well. Equation (6) shows that the visibility enhancement factor satisfies the inverse power law with (1-RH). The decrease of humidification factor with wavelength also shows that the visibility increases with the increase in wavelength. Equation (12) shows that the hygroscopic growth has satisfied the inverse power relation also with (1-RH) and the reciprocal of mean exponent of aerosol growth curve. It can also be said that for a fixed value of mean exponent of the aerosol growth curve μ, the humidification factor γ decreases with the increase in wavelength, this also shows that the visibility increases with the increase in wavelength (as the particles size decreases) i.e it satisfies the inverse power law of equation (6) and decreases with an increase in RH. Based on equation (9), the mean exponent of the aerosol size distribution (v) decrease with wavelength which shows that the number of larger particles increase compared to smaller particles and this is due to major coagulation amount caused by the increase in number of fine mode particles and consequently the tiny particles coagulate more than the larger particles as said by [29],[32]. It can also be noted from the values of (v) that the average atmospheric condition of the area is foggy [29].

Table 10 the results of the analysis of skewness and kurtosis using SPSS.

	Invis00	Invis50	Invis70	Invis80	Invis90	Invis95	Invis98	Invis99
Skewness	-0.8571	-1.6198	-1.0143	-1.0944	-0.5567	-0.2418	-0.2657	-0.3158
Kurtosis	-1.7143	0.7347	0.1852	0.6107	-0.6429	-0.7605	-1.1768	-0.9861

From Table 4, the behaviors and changes of particles size distribution are displayed in terms of vertical behavior (kurtosis) and horizontal behavior (skewness). From skewness, it can be seen that it is negative at all RHs, this implies that it is negatively skewed and this signifies that the particle distribution is dominated by coarse mode particles. From the kurtosis, it can be observed that it is also negative all through. and this shows that it is platykurtic, and the average vertical size distribution of the particles is below normal size distribution. The fluctuations in the values of the values of skewness and kurtosis maybe due to the nonlinear relation between the particles size distribution with RH and the physically mixed aerosols.

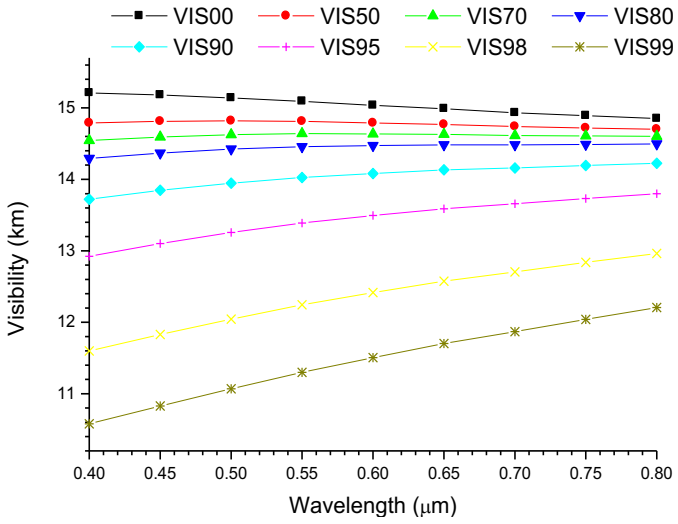

Fig. 4 a graph of visibility against wavelength for mian model 4

From Fig. 4, it can be observed that the visibility increases with the increase in wavelength, and decreases with the increase in relative humidity (RH). It can also be observed that the visibility is lower at shorter wavelengths with the maximum and minimum values of 15.1km and 10.8km which shows the dominance of coarse mode particles with some traces of fine

mode particles. It should also be noted that fine mode particles scatter and absorb more solar radiation than the coarse mode particles [31]. Since from equation (3) the visibility is the inverse of extinction, this implies that the visibility will be lower at shorter wavelengths. It can also be noted that the variation in the visibility at lower RHs (00-90) and higher wavelengths is very sharp but it is more pronounced at the higher RHs.

Table 11 Results of the regression analysis of equations (4) and (5) for visibility using SPSS.

	Linear			Quadratic			
RH	R^2	α	β	R^2	α_1	α_2	β
0%	0.907981	0.040390	0.265789	0.918619	0.06534	-0.02212	0.267367
50%	0.246149	0.007010	0.265766	0.526662	0.04971	-0.03787	0.268473
70%	0.366586	0.008555	0.266211	0.718639	0.03928	-0.04242	0.269250
80%	0.723547	0.018029	0.268122	0.782308	0.01129	-0.02600	0.269993
90%	0.924074	0.057627	0.270494	0.970533	0.01610	-0.06539	0.275268
95%	0.989085	0.059012	0.140796	0.989085	0.059012	-0.02923	0.278887
98%	0.995143	0.161022	0.290496	0.995637	0.181489	0.018151	0.289089
99%	0.997220	0.206233	0.305976	0.997282	0.196921	-0.00826	0.306653

By observing the R^2 values from both the linear and quadratic part of Table 11, it can be seen that the data fitted the equation models very well except at 50%RH, 70%RH and 80%RH. From the linear part, since α (angstrom exponent) is less than 1, this signifies the dominance of coarse mode particles. The increase of α with RH shows that coarse mode particles are being reduced from the atmosphere more than fine mode particles as a result of the increase in RH and also due to coagulation and sedimentation. Considering the quadratic part, it can be seen that α_2 is negative at all RHs except at 98%RH, and this shows monomodal distribution of coarse mode particles except at 98%RH which indicates bimodal type of distribution with coarse mode particles as dominant and traces of fine mode particles. The fluctuations in α_2 with RH shows the non-linearity relation between particles size distribution and RH and also with the physically mixed aerosols. The increase in turbidity coefficient β with RH signifies decrease in visibility with increase in RH.

Table 12 the result of the analysis of equations (8) and (12) using SPSS.

	μ	18.4427	
λ(m)	R^2	γ	v
0.55	0.941089	0.050582	1.932869
0.65	0.93228	0.0425	1.783815
0.75	0.92415	0.035938	1.662794

By observing the values of R^2, it can be said that the data fitted the equation models very well. Equation (6) shows that the visibility enhancement factor satisfies the inverse power law with (1-RH). The decrease of humidification factor with wavelength also shows that the visibility increases with the increase in wavelength. Equation (12) shows that the hygroscopic growth has satisfied the inverse power relation also with (1-RH) and the reciprocal of mean exponent of aerosol growth curve. It can also be said that for a fixed value of mean exponent of the aerosol growth curve μ, the humidification factor γ decreases with the increase in wavelength, this also shows that the visibility increases with the increase in wavelength (as the particles size decreases) i.e it satisfies the inverse power law of equation (6) and decreases with an increase in RH. Based on equation (9), the mean exponent of the aerosol size distribution (v) decrease with wavelength which shows that the number of larger particles increase compared to smaller particles and this is due to major coagulation amount caused by the increase in number of fine mode particles and consequently the tiny particles coagulate more than the larger particles as said by [29],[32]. It can also be noted from the values of (v) that the average atmospheric condition of the area is foggy [29].

Table 13 the results of the analysis of skewness and kurtosis using SPSS.

	Invis00	Invis50	Invis70	Invis80	Invis90	Invis95	Invis98	Invis99
Skewness	-0.1071	-3.0000	-3.0000	-0.8571	-0.9470	-0.4655	-0.2445	-0.3293
Kurtosis	-0.6429	9.0000	9.0000	-1.7143	-0.0179	-1.1852	-1.2438	-1.0385

From Table 13, the behaviors and changes of particles size distribution are displayed in terms of vertical behavior (kurtosis) and horizontal behavior (skewness). From skewness, it can be seen that it is negative from the RHs of 00 to 99%, this implies that it is negatively skewed and this signifies that the particle distribution is dominated by coarse mode particles. From the kurtosis, it can be observed that it is also negative all through. and this shows that it is platykurtic, and the average vertical size distribution of the particles is below normal size distribution. The fluctuations in the values of the values of skewness and kurtosis maybe due to the nonlinear relation between the particles size distribution with RH and the physically mixed aerosols.

INTERNATIONAL JOURNAL OF SCIENTIFIC & ENGINEERING RESEARCH, VOLUME 12, ISSUE 4, APRIL-2021
ISSN 2229-5518

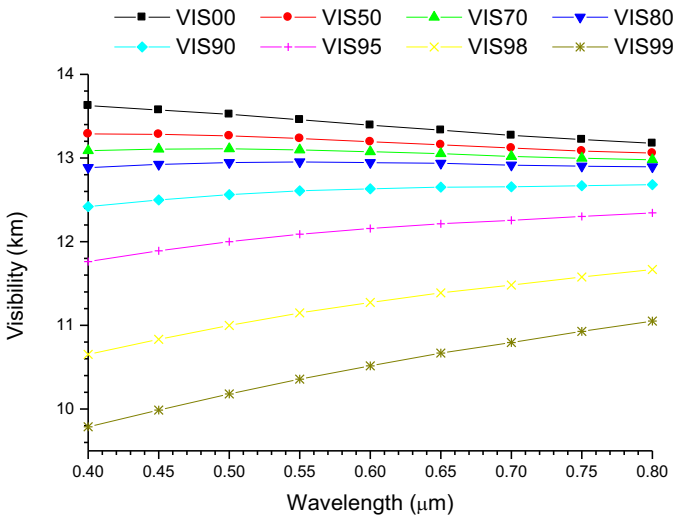

Fig. 5 a graph of visibility against wavelength for mian model 5

From Fig. 5, it can be observed that the visibility increases with the increase in wavelength, and decreases with the increase in relative humidity (RH). It can also be observed that the visibility is lower at shorter wavelengths with the maximum and minimum values of 13.7km and 9.9km which shows the dominance of coarse mode particles with some traces of fine mode particles. It should also be noted that fine mode particles scatter and absorb more solar radiation than the coarse mode particles [31]. Since from equation (3) the visibility is the inverse of extinction, this implies that the visibility will be lower at shorter wavelengths. From the plot, it can also be noted that the change in visibility at higher RHs (95-99) is more pronounced that at the lower RHs.

Table 14 Results of the regression analysis of equations (4) and (5) for visibility using SPSS.

	Linear			Quadratic			
RH	R^2	α	β	R^2	α_1	α_2	β
0%	0.989917	0.050140	0.299965	0.998573	0.076884	-0.023719	0.301875
50%	0.946324	0.027300	0.301026	0.994900	0.062587	-0.031293	0.303557
70%	0.776788	0.014020	0.301842	0.983921	0.055306	-0.036618	0.304814
80%	0.911052	0.000850	0.302870	0.952475	0.045521	-0.039617	0.306098
90%	0.912533	0.028500	0.305850	0.996723	0.020886	-0.043797	0.309455
95%	0.985004	0.068416	0.311398	0.999539	0.021004	-0.042047	0.314921
98%	0.997891	0.130839	0.325092	0.999878	0.097529	-0.029540	0.327671
99%	0.999852	0.175544	0.340265	0.999915	0.167644	-0.007006	0.340903

By observing the R^2 values from both the linear and quadratic part of Table 14, it can be seen that the data fitted the equation models very well except at 70%. From the linear part, since α (angstrom exponent) is less than 1, this signifies the dominance of coarse mode particles. The increase and fluctuations of α with RH shows that coarse mode particles are being reduced from the atmosphere more than fine mode particles as a result of the increase in RH due to coagulation and sedimentation. Considering the quadratic part, it can be seen that α_2 is negative all through the 8 RHs, and this shows monomodal distribution of coarse mode particles. The fluctuation in α_2 with RH shows the non-linearity relation between particles size distribution and RH and also with the physically mixed aerosols. The increase in turbidity coefficient β with RH signifies decrease in visibility with increase in RH.

Table 15 the result of the analysis of equations (8) and (12) using SPSS.

	μ	19.84442	
λ (m)	R^2	γ	v
0.55	0.938951	0.045545	1.903814
0.65	0.930398	0.038161	1.757283
0.75	0.922781	0.032141	1.637819

By observing the values of R^2, it can be said that the data fitted the equation models very well. Equation (6) shows that the visibility enhancement factor satisfies the inverse power law with (1-RH). The decrease of humidification factor with wavelength also shows that the visibility increases with the increase in wavelength. Equation (12) shows that the hygroscopic growth has satisfied the inverse power relation also with (1-RH) and the reciprocal of mean exponent of aerosol growth curve. It can also be said that for a fixed value of mean exponent of the aerosol growth curve μ, the humidification factor γ decreases with the increase in wavelength, this also shows that the visibility increases with the increase in wavelength (as the particles size decreases) i.e it satisfies the inverse power law of equation (6) and decreases with an increase in RH. Based on equation (9), the mean exponent of the aerosol size distribution (v) decrease with wavelength which shows that the number of larger particles increase compared to smaller particles and this is due to major coagulation amount caused by the increase in number of fine mode particles and consequently the tiny particles coagulate more than the larger particles as said by [29],[32]. It can also be noted from the values of (v) that the average atmospheric condition of the area is foggy [29].

Table 16 the results of the analysis of skewness and kurtosis using SPSS.

	Invis00	Invis50	Invis70	Invis80	Invis90	Invis95	Invis98	Invis99
Skewness	0.0349	-0.2742	-0.6116	-0.2653	-1.2498	-0.7096	-0.4576	-0.3394
Kurtosis	-1.4111	-1.5501	-1.2863	-1.4880	0.7426	-0.4678	-0.9003	-1.0344

From Table 16, the behaviors and changes of particles size distribution are displayed in terms of vertical behavior (kurtosis) and horizontal behavior (skewness). From skewness, it can be seen that it is negative from the natural log of visibility of at all RHs (00 to 99%), this implies that it is negatively skewed and this signifies that the particle distribution is dominated by coarse mode particles. From the kurtosis, it can

INTERNATIONAL JOURNAL OF SCIENTIFIC & ENGINEERING RESEARCH, VOLUME 12, ISSUE 4, APRIL-2021
ISSN 2229-5518

be observed that it is also negative all through. and this shows that it is platykurtic, and the average vertical size distribution of the particles is below normal size distribution. The fluctuations in the values of the values of skewness and kurtosis maybe due to the nonlinear relation between the particles size distribution with RH and the physically mixed aerosols.

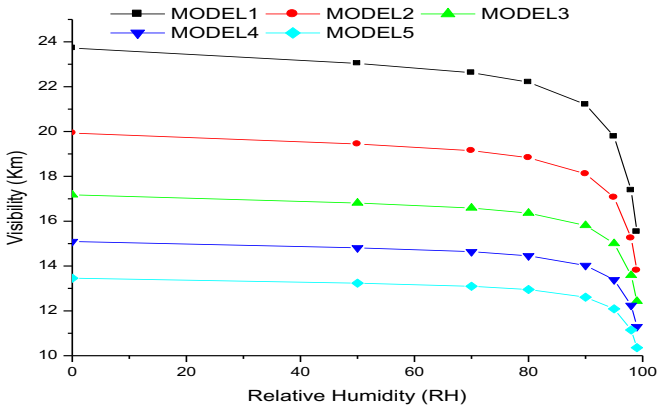

Fig. 6 plot of Visibility against Relative Humidity (RH%) at 0.55µm spectral wavelength (green) and varrying MIAN concentrartion

It can be observed from Fig. 6 that the visibility decrease with the increase in MIAN concentrations and also decresease with the increase in RH across the five models.

4.Summary

From the models considered, it was observed that:

I. the (α) angstrom exponent values are less than 1 throughout and increased for models 1 and 2 with the increase in RHs and aerosols concentrations while it fluctuates for models 3,4 and 5 respectively.

II. The curvature (α_2) is be observed to be monomodal type of distribution from 0-95% RH and bimodal distribution from 98-99% for model 1, monomodal from 00-98%RH and bimodal at 99%RH for model 2, monomodal (00-90 and at 99%RH) and bimodal (95% and 98%RH) for model 3, monomodal (00-95 and 99%RH) and bimodal at 98%RH, monomodal type of coarse mode particles distribution from 00-99%RH for model 5. Hence it can be said that the visibility decreases with the increase in RH and the increase in the concentration of MIAN

III. It can be observed that the turbidity coefficients β increase with the increase in RH across all the models, this implies that the visibility decreases with the increase in RH.

IV. Based on the results of the analysis of equations (6), (9), (12) and the plots of visibility against the wavelengths, it can be observed that there is an inverse relation between the humidification factor γ, the mean exponent of the aerosol size distribution ν with the particles concentration (i.e as the magnitudes of the humidification factor and the mean exponent of aerosol size distribution increase with the increase in the concentration of the particles and the increase in wavelengths across the models, the visibility decreases across the models). It can also be observed that as the magnitude of the mean exponent of aerosol growth curve (μ) increased with the increase in particles concentration and the increase of wavelengths across the models, the magnitudes of the humidification factor (γ) and the mean exponent of aerosol size distribution (ν) decreased across the models.

V. It can be observed that there are fluctuations in the magnitude of the skewness and kurtosis across the studied models. This may be due to the nonlinear relationship between the particle size distribution and the physically mixed aerosols with RH.

5.Conclusion

So, it can be concluded that, the visibility decreases with the increase in RHs, increase in MIAN (particles concentration) and with the increase in wavelengths. The decrease of visibility with the increase in MIAN concentration signifies that smaller particles have greater impact in visibility degradation. Also, the fluctuations in the magnitude of the values of (α) across the models and at all RHs implied coarse mode particles with some traces of fine mode particles. The increase in the magnitude of the curvature across the models with increase in concentration signifies that fine mode particles are becoming dominance over the coarse mode particles. The fluctuations of (α_2) as a result of the change in RHs and particle concentrations signifies nonlinear relationship between RHs and the physically mixed aerosols. It can also be concluded that the visibility decreased with the increase in the magnitudes of both the humidification factor (γ) and the mean exponent of aerosol size distribution (ν). there is a direct relationship between the mean exponent of aerosol size distribution, the humidification factor with the mean exponent of aerosol growth curve. Additionally, the fluctuations in the magnitude of skewness and kurtosis also signifies that there is dominance of coarse mode particles with some traces of fine mode particles across the models and that the relationship between the particles size distribution, RHs with the physically mixed aerosols is nonlinear.

References

[1] K. Megahed, “The Impact of Mineral Dust Aerosol Particles on Cloud Formation,” 2006.

[2] P. Srivastava, S. Dey, A. Kumar, S. Singh, S. K. Mishra, and S. Tiwari, “Science of the Total

Environment Importance of aerosol non-sphericity in estimating aerosol radiative forcing in Indo-Gangetic Basin," *Sci. Total Environ.*, vol. 599–600, pp. 655–662, 2017, doi: 10.1016/j.scitotenv.2017.04.239.

[3] S. K. Mishra, S. N. Tripathi, S. G. Aggarwal, and A. Arola, "Optical properties of accumulation mode, polluted mineral dust: Effects of particle shape, hematite content and semi-external mixing with carbonaceous species," *Tellus, Ser. B Chem. Phys. Meteorol.*, vol. 64, no. 1, 2012, doi: 10.3402/tellusb.v64i0.18536.

[4] S. R. Osborne, B. T. Johnson, J. M. Haywood, A. J. Baran, M. A. J. Harrison, and C. L. McConnell, "Physical and optical properties of mineral dust aerosol during the Dust and Biomass-burning Experiment," *J. Geophys. Res. Atmos.*, vol. 113, no. 23, pp. 1–14, 2008, doi: 10.1029/2007JD009551.

[5] A. Chemistry, P. Zieger, E. Weingartner, and U. Baltensperger, "Effects of relative humidity on aerosol light scattering : Results from different European sites Effects of relative humidity on aerosol light scattering : results from different European sites," no. April, 2013, doi: 10.5194/acp-13-10609-2013.

[6] J. H. Seinfeld and J. Wiley, *ATMOSPHERIC From Air Pollution to Climate Change SECOND EDITION*. 2006.

[7] P. Zieger *et al.*, "Revising the hygroscopicity of inorganic sea salt particles," *Nat. Commun.*, 2017, doi: 10.1038/ncomms15883.

[8] P. Zieger, R. Fierz-Schmidhauser, E. Weingartner, and U. Baltensperger, "Effects of relative humidity on aerosol light scattering: Results from different European sites," *Atmos. Chem. Phys.*, vol. 13, no. 21, pp. 10609–10631, 2013, doi: 10.5194/acp-13-10609-2013.

[9] G. Titos *et al.*, "Effect of hygroscopic growth on the aerosol light-scattering coefficient: A review of measurements, techniques and error sources," *Atmos. Environ.*, 2016, doi: 10.1016/j.atmosenv.2016.07.021.

[10] Y. Zhang and G. R. Carmichael, "The role of mineral aerosol in tropospheric chemistry in East Asia-a model study," *J. Appl. Meteorol.*, vol. 38, no. 3, pp. 353–366, 1999, doi: 10.1175/1520-0450(1999)038<0353:TROMAI>2.0.CO;2.

[11] P. Tsilimigras, "On the applicability of the Roothaan-Bagus procedure," *Chem. Phys. Lett.*, vol. 11, no. 1, pp. 99–100, 1971, doi: 10.1016/0009-2614(71)80541-9.

[12] R. J. Charlson, "current research," vol. 3, no. 10, pp. 913–918, 1969.

[13] and I. schult M. Hess, P. Koepke, "Optical Properties of Aerosols and Clouds: The Software Package OPAC," pp. 831–844, 1998.

[14] K. K. Moorthy, A. Saha, B. S. N. Prasad, K. Niranjan, D. Jhurry, and P. S. Pillai, "Aerosol optical depths over peninsular India and adjoining oceans during the INDOEX campaigns: Spatial, temporal, and spectral characteristics," *J. Geophys. Res. Atmos.*, vol. 106, no. D22, pp. 28539–28554, 2001, doi: 10.1029/2001JD900169.

[15] S. Singh, S. Nath, R. Kohli, and R. Singh, "Aerosols over Delhi during pre-monsoon months : Characteristics and effects on surface radiation forcing," vol. 32, pp. 4–7, 2005, doi: 10.1029/2005GL023062.

[16] E. L. Koschmieder, "Symmetric Circulations of Planetary Atmospheres," *Adv. Geophys.*, vol. 20, no. C, pp. 131–181, 1978, doi: 10.1016/S0065-2687(08)60323-4.

[17] M. D. and D. M. B. King, "a method for inferring total ozone content from spectral variation of total optical depth obtained with solar radiometer." 1976.

[18] B. I. Tijjani, F. Sha'aibu, and A. Aliyu, "The Effect of Relative Humidity on Maritime Tropical Aerosols," *Open J. Appl. Sci.*, vol. 04, no. 06, pp. 299–322, 2014, doi: 10.4236/ojapps.2014.46029.

[19] B. I. Tijjani, F. Sha'aibu, and A. Aliyu, "The Effect of Relative Humidity on Maritime Polluted Aerosols," *Open J. Appl. Sci.*, vol. 04, no. 06, pp. 299–322, 2014, doi: 10.4236/ojapps.2014.46029.

[20] N. T. O'Neill, O. Dubovik, and T. F. Eck, "Modified Ångström exponent for the characterization of submicrometer aerosols," *Appl. Opt.*, vol. 40, no. 15, p. 2368, 2001, doi: 10.1364/ao.40.002368.

[21] N. T. O'Neill, T. F. Eck, A. Smirnov, B. N. Holben, and S. Thulasiraman, "Spectral discrimination of coarse and fine mode optical depth," *J. Geophys. Res. D Atmos.*, vol. 108, no. 17, pp. 1–15, 2003, doi: 10.1029/2002jd002975.

[22] J. Kaufman, "Aerosol Optical Thickness and Atmospheric Path Radiance," vol. 98, pp. 2677–2692, 1993.

[23] T. F. Eck, B. N. Holben, A. Smirnov, I. Slutsker, J. M. Lobert, and V. Ramanathan, "Column-integrated aerosol optical properties over the Maidives during the northeast," vol. 106, 2001.

[24] J. S. Reid, A. Smirnov, N. T. O. Neill, I. Slutsker, and S. Kinne, "In / X," vol. 104, no. 1, 1999.

[25] T. F. Eck *et al.*, "Characterization of the optical properties of biomass burning aerosols in Zambia during the 1997 ZIBBEE field campaign," vol. 106,

pp. 3425–3448, 2001.

[26] F. Kasten, "Visibility forecast in the phase of pre-condensation," *Tellus*, vol. 21, no. 5, pp. 631–635, Jan. 1969, doi: 10.3402/tellusa.v21i5.10112.

[27] B. I. Tijjani, "The Effect of Soot and Water Soluble on the Hygroscopicity of Urban Aerosols," vol. 26, pp. 52–73, 2013, [Online]. Available: www.iiste.org.

[28] P. K. Quinn *et al.*, "Impact of particulate organic matter on the relative humidity dependence of light scattering: A simplified parameterization," *Geophys. Res. Lett.*, vol. 32, no. 22, pp. 1–4, 2005, doi: 10.1029/2005GL024322.

[29] Junge et. al., "Chapter 2 Physical and Optical properties of aerosols," no. 1, 1958.

[30] S. Sjogren, M. Gysel, E. Weingartner, U. Baltensperger, M. J. Cubison, and H. Coe, "Hygroscopic growth and water uptake kinetics of two-phase aerosol particles consisting of ammonium sulfate , adipic and humic acid mixtures," vol. 38, pp. 157–171, 2007, doi: 10.1016/j.jaerosci.2006.11.005.

[31] E. Swietlicki *et al.*, "Hygroscopic properties of submicrometer atmospheric aerosol particles measured with H-TDMA instruments in various environments - A review," *Tellus, Ser. B Chem. Phys. Meteorol.*, vol. 60 B, no. 3, pp. 432–469, 2008, doi: 10.1111/j.1600-0889.2008.00350.x.

[32] R. Lang and N. X. Xanh, "Smoluchowski's theory of coagulation in colloids holds rigorously in the Boltzmann-Grad-limit," *Zeitschrift für Wahrscheinlichkeitstheorie und Verwandte Gebiete*, vol. 54, no. 3, pp. 227–280, 1980, doi: 10.1007/BF00534345.